Journal of the European Ceramic Society **6** (1990) 129–135

Influence of Microstructure on the Superconducting Properties of Polycrystalline $YBa_2Cu_3O_{7-x}$

Mesut Aslan, Herbert Jaeger, Gerhard Kaiser, Rose Gröner, Klaus Schulze* & Günter Petzow

Max-Planck-Institut für Metallforschung, Institut für Werkstoffwissenschaft, Pulvermetallurgisches Laboratorium, D-7000 Stuttgart 80, FRG

(Received 19 January 1990; revised version received 28 February 1990; accepted 15 March 1990)

Abstract

Microstructural development and shrinkage during sintering of $YBa_2Cu_3O_{7-x}$ is determined not only by the sintering parameters but also by the starting components and calcination procedure. During sintering the residual carbonate content in calcined powders causes gas porosity and inhomogeneous microstructural development. Small amounts of second phases lead to reduced sintering rate. The critical current density of sintered samples is related to the average grain size. A fine-grained microstructure enhances the current transport capability remarkably. After identical post-annealing treatment, fine-grained samples show comparatively higher values of oxygen concentration. The enhancement of critical current density by a fine-grained microstructure is traced back to the favorable distribution of the non-superconducting phases present, fewer cracks, and an increased and more homogeneous oxygen concentration.

Die Gefügeentwicklung und Verdichtung während des Sinterns von $YBa_2Cu_3O_{7-x}$ wird nicht nur durch die Sinterbedingungen sondern auch durch die Ausgangsmaterialien und die Kalzinierung beeinflußt. Der in kalzinierten Pulvern zurückgebliebene Anteil an Karbonaten verursacht während des Sinterns Porosität und führt zu einer inhomogenen Gefügeentwicklung. Geringe Mengen einer zweiten Phase führen zu einer Abnahme der Sinterrate. Die kritische Stromdichte gesinterter Proben hängt von der durchschnittlichen Korngröße ab. Ein feinkörniges Gefüge erhöht das Stromtransportvermögen beträchtlich. Feinkörnige Proben zeigen nach identisch durchgeführter nachträglicher Wärmebehandlung vergleichsweise höhere Sauerstoffkonzentrationen. Die Erhöhung der kritischen Stromdichte feinkörniger Gefüge wird auf eine vorteilhafte Verteilung der vorhandenen nicht supraleitenden Phasen, weniger Risse und einen erhöhten und homogener verteilten Sauerstoffgehalt zurückgeführt.

Le développement de la microstructure et le retrait durant le frittage de l'$YBa_2Cu_3O_{7-x}$ ne sont pas déterminés uniquement par les paramètres de frittage, mais également par les constituants de départ et le procédé de calcination. Lors du frittage, le carbonate résiduel contenu dans les poudres calcinées provoque une porosité de gaz et le développement d'une microstructure non homogène. Le frittage est ralenti par de petites quantités de phases secondaires. La densité critique de courant des échantillons frittés dépend de la taille moyenne des grains. Une microstructure fine améliore sensiblement l'aptitude au transport du courant. Après recuit, les concentrations en oxygène le plus élevées sont observées pour les échantillons à grains fins. L'amélioration de la densité critique de courant dans le cas d'une microstructure fine est attribuée à une bonne répartition des phases non supraconductrices, à une réduction du nombre de fissures et à l'oxygène, qui est mieux réparti et en plus forte concentration.

1 Introduction

In spite of new ceramic superconductors based on Bi and Tl, with critical temperatures of 110 and 125 K, the compound $YBa_2Cu_3O_{7-x}$ is still attractive for technical applications. For production of functional parts the powder metallurgical (P/M) route is the

* To whom all correspondence should be addressed.

Journal of the European Ceramic Society 0955-2219/90/$3.50

most suitable. Therefore knowledge of the sintering mechanisms and microstructural control during sintering is of practical interest. The shrinkage of powders during sintering is influenced by a number of parameters such as surface energy and diffusion and creep constants; in addition, the morphology of powders (particle size, particle size distribution, surface properties) and the initial powder packing (density, homogeneity) play an important role. In most cases, the dislocation mobility in ceramic materials is very low because of the directional bonding. Thus shrinkage and pore elimination during sintering occurs mainly by diffusion or diffusion-controlled mechanisms. Finer starting powders yield shorter diffusion distances. Therefore, to achieve optimal sintering behavior, powders of small particle size should be used.

The quality of the superconducting materials is determined not only by critical temperature, workability and mechanical strength but also by the current transport capability in the presence of a magnetic field. The critical current density measured on single crystals and epitaxially grown textured thin film reaches values up to 10^7 A/cm^2 at 77 K and in zero magnetic field.[1-3] Under the same conditions, melt-textured polycrystalline samples show values of J_c as high as 7×10^4 A/cm^2.[4,5] However, for high magnetic field applications, bulk materials produced by powder metallurgical methods are necessary. Up to now the great disadvantage of sintered polycrystalline $YBa_2Cu_3O_{7-x}$ is the low critical current density and its strong decrease under external magnetic fields. Because of the anisotropic nature of electrical properties and a short coherence length, intrinsic and extrinsic defects in the microstructure have detrimental effects on the critical current density. Among these defects are twin boundaries, grain boundaries, insulating grain boundary phases, pores, cracks originating from the tetragonal/orthorhombic phase transformation, and defects on an atomic scale, such as stacking faults and incomplete or inhomogeneous oxygen content.

2 Experiments

Powders of the nominal composition $YBa_2Cu_3O_{7-x}$ from the starting materials Y_2O_3, BaO, $BaCO_3$ and CuO were prepared by mixing and calcining the mixtures at 880 and 900°C. Before calcining, the powders were mixed intimately by two different methods. Initially, all powders were mixed in a tumbler in isopropanol with intermediate ultrasonic treatment and then dried in a rotary vaporizer. For powder mixtures containing BaO, homogenization in isopropanol slurry resulted in powders of low sinterability. Therefore such powder mixtures were dry-milled in an agate ball mill for 10 min, and sieved. The homogenized powders were then calcined twice at 880 and 900°C for 10 h with an intermediate grinding. After calcining, the powders were again ball milled for 10 min, and sieved. The average particle size of the powders was between 1·5 and 2·5 μm. A detailed description of the powder preparation is given in Ref. 6.

The calcined powders were pressed isostatically at 630 MPa into small cylindrical pellets (dia. 5 mm, length 12 mm) and sintered in a muffle furnace in air at 950°C for 1–20 h. The heating and cooling rates were 10 and 5 K/min, respectively. After sintering, the samples prepared with BaO showed mainly closed porosity (relative density $D > 0{\cdot}93$), and the oxygen uptake during cooling was insufficient for a complete transformation from the tetragonal phase to the superconducting orthorhombic phase. Hence the samples were post-annealed at 400°C in air and in flowing oxygen for between 5 and 20 h. The critical current density and critical temperature were measured by a standard four-probe technique. The oxygen content of sintered and post-annealed samples was determined by the carrier gas hot extraction method using a Leco TC436 analyser. For that purpose a small amount of the samples (1–4 mg) was put into Ni hulls and placed in a graphite crucible which then was heated resistively to 2200°C. The sample decomposes and the free oxygen reacts with the graphite to form CO; this in turn oxidizes to CO_2, which is detected in an IR-absorption cell.

For metallographic examination the samples were embedded in epoxy, dry-ground on SiC paper and polished in SiO_2 suspension on a vibrating polisher.[7,8] The average grain size of the samples was measured by linear intercept analysis.

3 Results

Figure 1 shows the relative density of samples produced with $BaCO_3$ and BaO after sintering at 950°C between 30 and 600 min. '$BaCO_3$ samples' have 5–7% higher porosity than the 'BaO samples'. The effect of an increased sintering time on the relative density is negligible.

The shrinkage during sintering appears to be very sensitive to small variations during powder processing and sintering, so that samples made from the same starting materials and produced under identical conditions show different values of relative

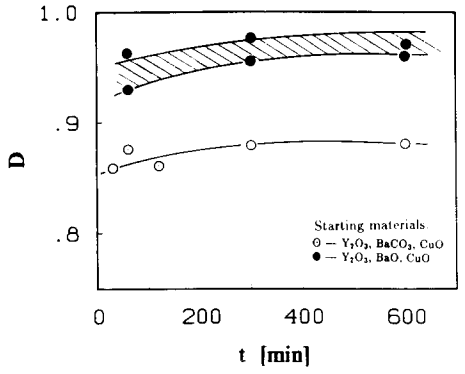

Fig. 1. Relative density D versus isothermal sintering time t at 950°C in air (post-annealing at 400°C for 5 h).

density. Figure 1 shows this for 'BaO samples' from two powder batches. The hatched area illustrates the width of the variation in relative density.

Figure 2 shows the influence of starting materials $BaCO_3$ and BaO on the microstructural development during sintering at 950°C for 5 h. The '$BaCO_3$ sample' contains noticeable amounts of second phases (Fig. 2(a), bright areas are CuO) and large

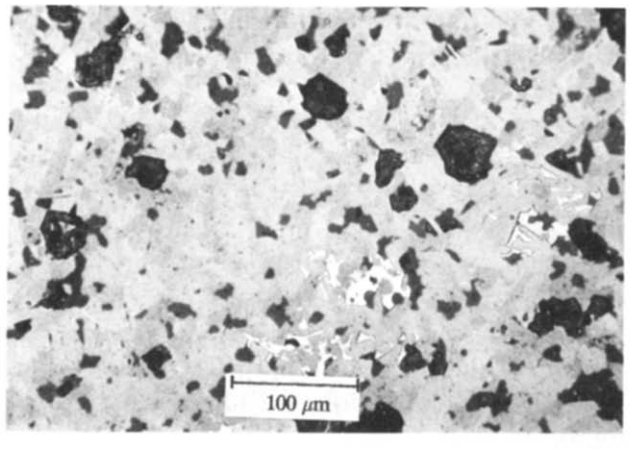

(a)

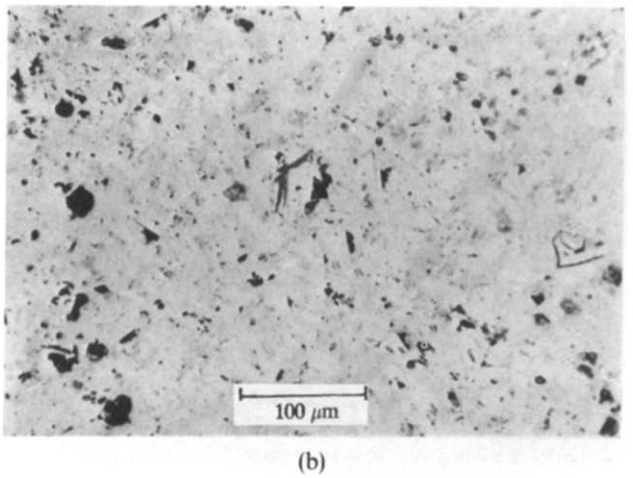

(b)

Fig. 2. Microstructure of $YBa_2Cu_3O_{7-x}$—samples sintered at 950°C for 5 h (bright field). (a) Starting materials Y_2O_3, $BaCO_3$ and CuO; (b) starting materials Y_2O_3, BaO and CuO.

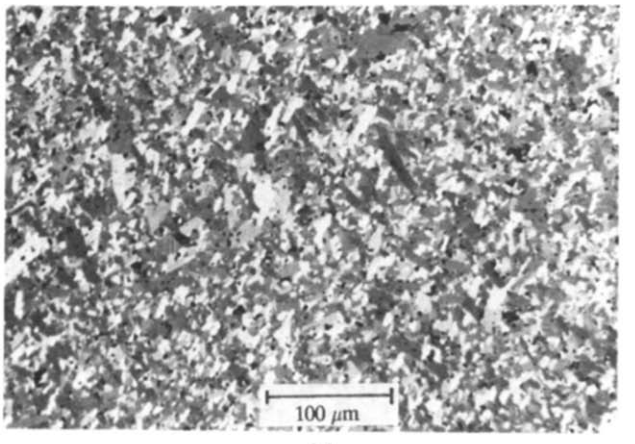

(a)

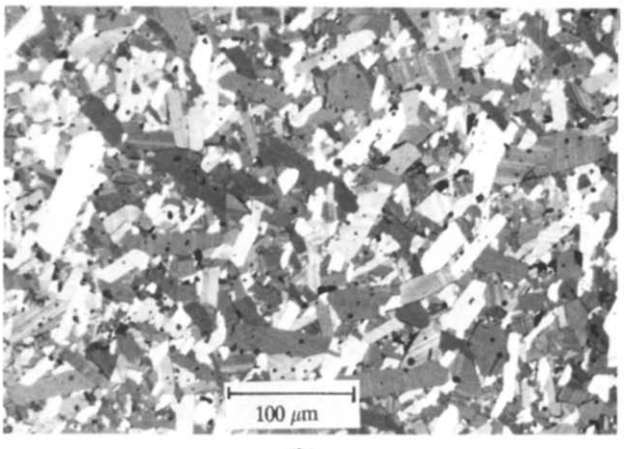

(b)

Fig. 3. Microstructural development of $YBa_2Cu_3O_{7-x}$—samples after sintering in air at 950 C for (a) 1 h and (b) 5 h (polarized light).

nearly spherical pores, which are believed to be due to the decomposition of residual $BaCO_3$ to BaO and CO_2. The 'BaO sample' shows considerably less porosity, and the pores are distributed homogeneously. The amount of optically visible second phases is very small (Fig. 2(b)).

The microstructure of the 'BaO samples' sintered at 950°C for 1 and 5 h and post-annealed at 400°C for 5 h is shown in Fig. 3(a) and (b). After sintering for 1 h, a fine-grained microstructure with average grain size of 3 μm is observed. The increase in sintering time to 5 and 10 h results in a significant coarsening of the microstructure. Sintering for more than 5 h causes negligible grain growth (average grain size 7·5 and 8·2 μm after sintering for 5 and 10 h, respectively). The grains show a plate-like morphology due to the anisotropic grain growth. Grain growth occurs in the crystallographic *a–b* directions and the grains are strongly twinned. In addition to regular pores at grain junctions and grain boundaries there exist pores in the grain interior, which were enclosed during grain growth.

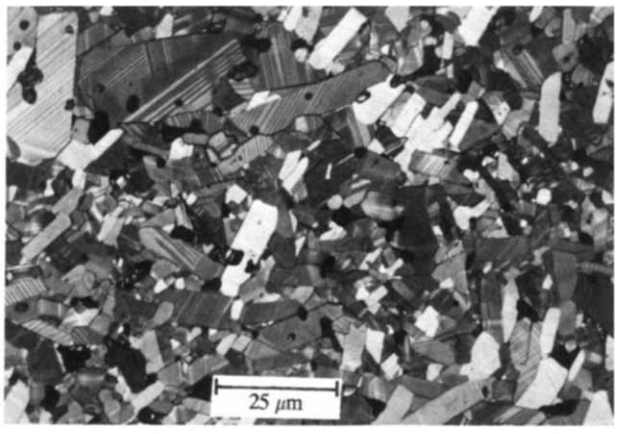

(a)

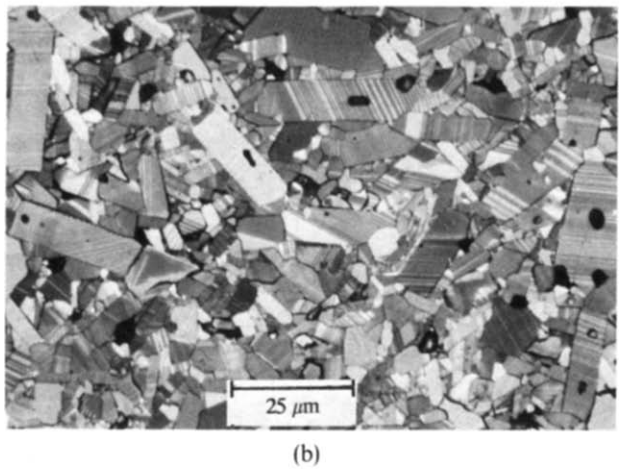

(b)

Fig. 4. Microstructure of $YBa_2Cu_3O_{7-x}$ after sintering and post-annealing at 400°C for (a) 5 h and (b) 10 h (samples were sintered at 950°C for 1 h, polarized light).

Some of the grains contain cracks, most pronounced in the sample sintered for 5 h (Fig. 3(b)).

Some grains in samples sintered at 950°C for 1 h and post-annealed at 400°C for 5 and 10 h are not twinned or are only partially twinned, as can be seen in Fig. 4(a) and (b). This indicates inhomogeneous oxygen content and incomplete formation of the superconducting orthorhombic phase. During post-annealing, no grain growth occurs, as can be seen by the similar average grain size of samples post-annealed for 5 and 10 h ($\bar{G} = 2{\cdot}6\ \mu m$).

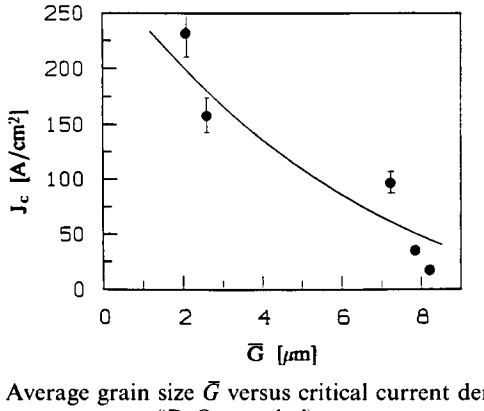

Fig. 5. Average grain size $\bar{G}$ versus critical current density J_c ('BaO samples').

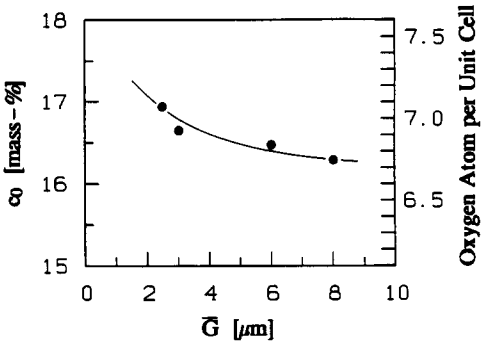

Fig. 6. Oxygen content c_0 versus average grain size $\bar{G}$ ('BaO samples' were sintered at 950°C for different times and post-annealed in air at 400°C for 15 h).

The oxygen content and critical current density of samples sintered at 950°C for different times and post-annealed at 400°C for 15 h in air increases with decreasing average grain size (Figs 5 and 6).

Figure 7 shows the microstructure of a sample which was post-annealed at 400°C for prolonged time. The strongly deteriorated grain boundaries, which indicate the decomposition of $YBa_2Cu_3O_{7-x}$, are noticeable.

The oxygen uptake on cooling leads to a tetragonal/orthorhombic (T/O) phase transformation combined with a decrease of the unit cell volume. Lattice strains due to this transformation are reduced by twinning in the orthorhombic phase and crack formation. In some cases, radial cracks may arise because the transformation propagates from the sample surface, and near-surface regions transformed already are subjected to tensile stress (see Fig. 8).

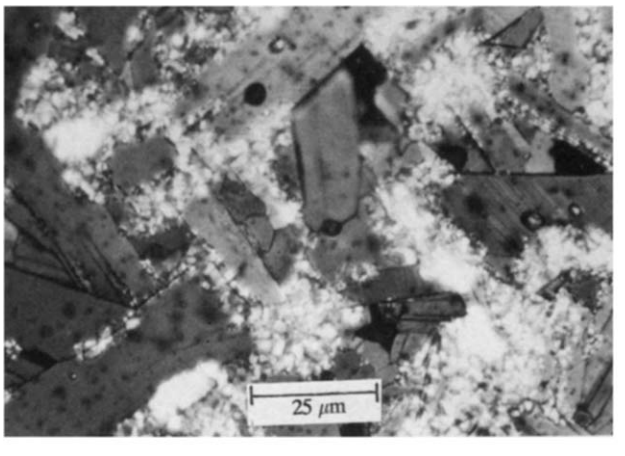

Fig. 7. Typical microstructure of $YBa_2Cu_3O_{7-x}$—sample post-annealed at 400°C for prolonged time ('BaO sample', polarized light).

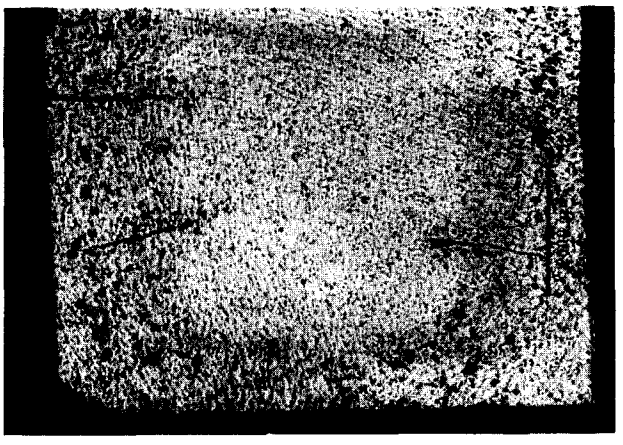

Fig. 8. Formation of radial cracks in sintered $YBa_2Cu_3O_{7-x}$ ('BaO sample'; the O/T-phase boundary can be distinguished by the difference in contrast).

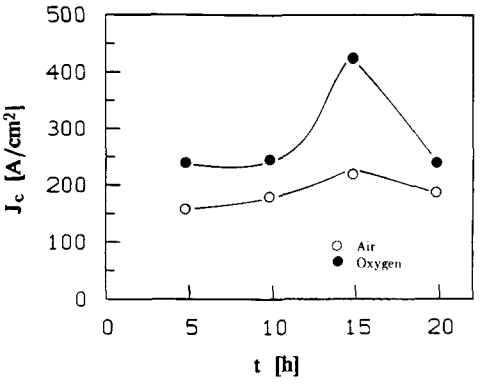

Fig. 9. Influence of post-annealing time at 400 °C on the critical current density J_c ('BaO sample', $\bar{G} = 2{\cdot}6\,\mu m$).

4 Discussion

The sintering experiments carried out in this work show that the shrinkage and pore elimination during sintering is strongly affected by small amounts of second phases in the starting powders. The effect of these second phases is more pronounced when their decomposition results in gaseous products during sintering, such as CO_2 and H_2O (from residual $BaCO_3$ and $Ba(OH)_2$). Because of the slow decomposition of $BaCO_3$ at calcination temperatures of 900°C, residual $BaCO_3$ is observed in powders from $BaCO_3$-containing precursors, even after repeated calcination steps. During sintering with closed porosity, the development of CO_2 leads to swelling and causes gas porosity. In this sintering stage shrinkage by diffusion or diffusion-controlled mechanisms may be inhibited by second phases (e.g. green phase Y_2BaCuO_5) at grain boundaries in the form of fine particles. Shrinkage during sintering proceeds by removing the layers from the particle contacts atom by atom and transporting them to the contact necks under the gradient of chemical potential. Because of the threshold potential introduced by second phases at grain boundaries and neck areas, the chemical potential gradient between the vacancy sources (neck areas) and sinks (grain boundaries at particle contacts) is reduced and the rate of sintering is decreased.[9]

The critical current density J_c of the sintered $YBa_2Cu_3O_{7-x}$ samples first increases with increasing post-annealing time at 400°C. For annealing times above 15 h a decrease of J_c is observed, as shown in Fig. 9. The decrease of J_c is more pronounced in samples post-annealed in flowing oxygen, because of their relatively high critical current density after an annealing time of 15 h.

Figure 10 shows the resistivity vs temperature plots of samples post-annealed in flowing oxygen with onset temperature of 93 K and transition width of 4 K. After post-annealing for longer than 15 h the normal state resistivity increases, and the critical current density decreases.

As is shown in Fig. 5, a fine-grained microstructure results in a higher critical current density. Similar results were reported in the literature for $(La_{1-x}Sr_x)_2CuO_4$ and $YBa_2Cu_3O_{7-x}$.[10,11] Recently, Smith *et al.* also have pointed out the role of grain size on the critical current density of $YBa_2Cu_3O_{7-x}$.[12] In our results the enhancement of the critical current density by a fine-grained microstructure is traced back to a more favorable distribution of non-superconducting grain boundary phases, inhibited crack formation, and more homogeneous and increased oxygen content.

The preparation of single-phase $YBa_2Cu_3O_{7-x}$ is not trivial because of a very narrow homogeneity range. Starting compositions with small local variation from the stoichiometry cause the formation of additional phases according to the phase

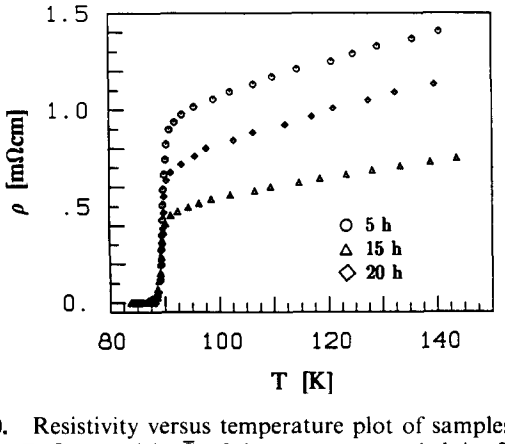

Fig. 10. Resistivity versus temperature plot of samples from Fig. 8 ('BaO sample', $\bar{G} = 2{\cdot}6\,\mu m$, post-annealed in flowing oxygen).

diagram.[13,14] In fine-grained samples the non-superconducting phases present are distributed over large grain surfaces, and thus their 'weak-link' effect is diminished.

The T/O phase transformation is accompanied by crack formation. The propagation of cracks in a matrix is determined by the average grain size, among other factors. As the cracks in the finer matrix are deflected more frequently over a given distance, the growth velocity of cracks is limited because of increased energy dissipation.[15] Thus, the crack-induced reduction of the sample cross-section is reduced, resulting in a higher critical current density.

The increase of critical current density by post-annealing in flowing oxygen can be explained by a more homogeneous oxygen distribution in samples. The critical current density decreases after prolonged post-annealing times at 400°C, whereas the normal state resistivities of the samples are increasing, as shown in Fig. 10. According to Roth *et al.*,[14] the compound $YBa_2Cu_3O_{7-x}$ decomposes in the components Y_2O_3, BaO and CuO during annealing below 700°C in oxygen-containing atmospheres.[13] Therefore the decrease of critical current density and increase of normal state resistivity can be traced back to the decomposition of $YBa_2Cu_3O_{7-x}$. Thus, considering the decomposition tendency of $YBa_2Cu_3O_{7-x}$, the post-annealing should be optimized to times as short as possible.

The maximum oxygen content of $YBa_2Cu_3O_7$ is 16·81 mass%. Measured oxygen contents above this value indicate possible systematic errors in the oxygen determination. As the mass of the samples to be analyzed lies between 1 and 4 mg, very homogeneous samples are necessary for accurate determination of the oxygen content. Different phases and substances present in the samples, such as carbonates, water and carbon, and their inhomogeneous distribution, may lead to strongly scattered results (standard deviation, $s_{rel} = \pm 4\%$ at oxygen contents of 16·5 mass%). For correct oxygen balance the oxygen content of carbonates, hydroxides and water must be taken into account, as they do not belong to the oxygen balance of $YBa_2Cu_3O_{7-x}$. During powder preparation and sintering of BaO-containing precursors the absorption of CO_2 and its reaction with BaO to $BaCO_3$ may cause formation of intergrain carbonates (Fig. 11(a)). During preparation of powder samples from the bulk by grinding with mortar and pestle the powders may be contaminated because of abrasion. Additional H_2O and CO_2 are absorbed from the ambient, which leads to formation of carbonates and hydroxides.

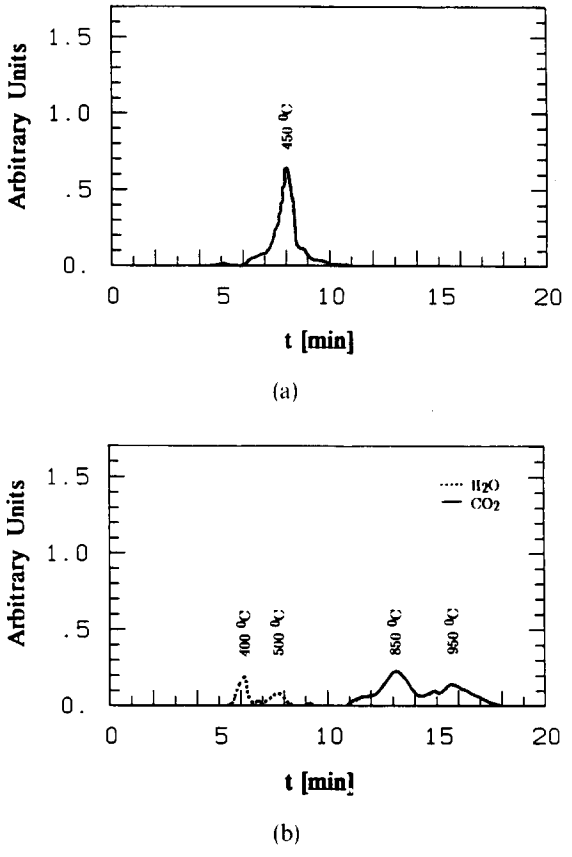

Fig. 11. Release of (a) $C(CO_2)$ and (b) CO_2 and H_2O from $YBa_2Cu_3O_{7-x}$.

Such oxygen sources can be distinguished and determined separately by various methods. For a reliable analysis the determination of CO_2 from C and CO_3 (present as residual carbonates) and H_2O is necessary. The determination of CO_2 and H_2O was achieved by slowly heating samples of 50–200 mg weight to 1200°C in N_2. The CO_2 and H_2O released by the sample is then detected by IR CO_2 and H_2O absorption cells (Fig. 11(b)). Free graphite contamination is burned out to CO_2 in flowing oxygen atmosphere and determined also by IR absorption spectroscopy (Fig. 11(a)). Taking these possibilities into account and repeating the analyses a number of times for improved statistics, the random errors can be reduced to typically 1%. As only small quantities of the samples were available, the number of O determinations per sample was limited to four and the number of C determinations per sample to one or two. The results of the oxygen analyses are compiled in Fig. 6; the relative error is 1·5–2·0%. The grain size dependence of oxygen concentration indicates the grain boundary diffusion to be the dominant mechanism of oxygen uptake. As the analysed samples have relative densities above 0·94 (closed porosity) the effect of an increased oxygen diffusion through the pore channels is negligible.

5 Conclusions

Microstructural control during sintering of polycrystalline $YBa_2Cu_3O_{7-x}$ plays a key role in improvement of the current transport capability. Because of the physical properties of the material, such as short coherence length and anisotropy of electrical conductivity, grain boundaries have to be free of insulating second phases and good intergrain integrity must be guaranteed. Therefore, the use of high-quality phase pure powders is essential. The phase purity of the powders is determined by the starting components and the calcination procedure. Porosity, grain size and oxygen content can be adjusted during sintering and subsequent annealing. Post-sinter annealing at 400°C in flowing oxygen is required for complete oxygenation of the samples. The increase of the oxygen partial pressure during post-annealing yields a more homogeneous oxygen distribution. As $YBa_2Cu_3O_{7-x}$ decomposes during prolonged heat treatments below 700°C, there is an optimal annealing time beyond which the critical current density starts to decrease. The relation between average grain size and oxygen concentration indicates that grain boundary diffusion is the dominant mechanism of oxygen uptake. Determination of the oxygen content by carrier gas hot extraction must be accompanied by a determination of CO_2 and H_2O to correct for oxygen balance due to the residual carbonates, as well as adsorbed CO_2 and H_2O from the ambient.

References

1. Worthington, T. K., Gallagher, W. J. & Dinger, T. R., Anisotropic nature of high-temperature superconductivity in single crystal $YBa_2Cu_3O_{7-x}$. *Phys. Rev. Lett.*, **59**(10) (1987) 1160–3.
2. Dinger, T. R., Worthington, T. K., Gallagher, W. J. & Sandstrom, R. L., Direct observation of electronic anisotropy in single crystal $YBa_2Cu_3O_{7-x}$. *Phys. Rev. Lett.*, **58**(25) (1987) 2687–90.
3. Chaudhari, P., Koch, R. H., Laibowitz, R. B., McGuire, T. R. & Gambino, R. J., Critical current measurements in epitaxial films of $YBa_2Cu_3O_{7-x}$ compound. *Phys. Rev. Lett.*, **58** (1987) 2684–7.
4. Jin, S., Tiefel, T. H., Sherwood, R. C., van Dover, R. B., Davis, M. E., Kammlot, G. W. & Fastnacht, R. A., Melt-textured growth of polycrystalline $YBa_2Cu_3O_{7-x}$ with high transport J_c at 77 K. *Phys. Rev.*, B, **37**(18) (1988) 7850–3.
5. Salama, K., Selvamanickam, V., Gao, L. & Sun, K., High current density in bulk $YBa_2Cu_3O_{7-x}$ superconductor. *Appl. Phys. Lett.*, **54**(23) (1989) 2352–4.
6. Jaeger, H., Aslan, M., Schulze, K., Bohsman, M. & Petzow, G., Microstructural optimization of superconducting oxides. *cfi/Ber. DKG*, **66**(3/4) (1989) 108–12.
7. Schäfer, U., Müller, G., Jaeger, H. & Schulze, K., Microstructure and characterisation of the ceramic high-T_c superconductor $YBa_2Cu_3O_{7-x}$. *Prakt. Met.*, **25** (1988) 488–94.
8. Schäfer, U., Müller, G., Jaeger, H., Aslan, M. & Schulze, K., Note on paper 'Microstructure and characterisation of the ceramic high-T_c superconductor $YBa_2Cu_3O_{7-x}$'. *Prakt. Met.*, **25** (1988) 610–11.
9. Ashby, M. F., Bahk, S., Bevk, J. & Turnbull, D., The influence of a dispersion of particles on the sintering of metal powders and wires. In *Progress in Materials Science*, Vol. 25, ed. J. W. Christian, P. Haasen & T. B. Massalski. Pergamon Press, Oxford, 1980, pp. 1–34.
10. Chiang, Y. M., Rudman, D. A., Leung, D. K., Ikeda, J. A. S., Roshko, A. & Fabes, B. D., Effect of grain size and grain boundary segregation on superconducting properties of dense polycrystalline $La_{1.85}Sr_{0.15}CuO_4$. *Physica*, C, **152** (1988) 77–90.
11. Chiang, Y. M., Ikeda, J. A. S. & Roshko, A., Grain boundary segregation and critical current density in $YBa_2Cu_3O_{7-x}$ superconductors. In *Ceramic Superconductors II*, ed. M. F. Yan. American Ceramic Society, Westerville, OH, 1988, pp. 607–18.
12. Smith, D. S., Suasmoro, I. & Gault, C., Demonstration of grain growth induced microcracking and its role for the electrical response of $YBa_2Cu_3O_{7-x}$. *J. Eur. Ceramic Soc.*, **5** (1989) 81–5.
13. Osamura, K., Zhang, W., Yamashita, T., Ochiai, S. & Predel, B., Phase equilibria around the superconducting phase in the BaO–Y_2O_3–CuO system. *Z. Metallkd.*, **79** (1988) 693–7.
14. Roth, R. S., Rawn, C. J., Beech, F., Whitler, J. D. & Anderson, J. O., Phase equilibria in the system Ba–Y–Cu–O–CO_2 in air. In *Ceramic Superconductors II*, ed. M. F. Yan. American Ceramic Society, Westerville, OH, 1988, pp. 13–26.
15. Rice, R. W., Freiman, S. W. & Becher, P. F., Grain-size dependence of fracture energy in ceramics: I, Experiments; II, A model for noncubic materials. *J. Am. Ceram. Soc.*, **64**(6) (1981) 345–54.